Effect of Nucleation Mechanism on Complex Poly(L-lactide) Nonisothermal Crystallization Process, Part 2: Crystallization Kinetics Analysis

Andrea Martinelli, Massimo Calì, Lucio D'Ilario, Iolanda Francolini, Antonella Piozzi

Dipartimento di Chimica, Sapienza Università di Roma, P.le A. Moro 5, Roma 00185, Italy

Received 30 October 2010; accepted 4 May 2011
DOI 10.1002/app.34833
Published online 31 August 2011 in Wiley Online Library (wileyonlinelibrary.com).

ABSTRACT: In the first part of this article, we reported the crystalline memory effect on the nonisothermal crystallization of poly(L-lactide). The experiments were carried out by using polymer single crystals growth from dilute solution as standard starting material. In this article (Part II), we have analyzed in detail the effect of the melting condition on the overall crystallization kinetics by applying the Nakamura-Avrami model to DSC results. The absence or the low concentration of foreign infusible heterogeneous nuclei in our system allowed us to exalt the self-nuclei role in polymer crystallization, to follow their concentration decrease during the melting process and to find the limiting melting temperature for their disappearance. Below such a temperature, a stable equilibrium number of self-nuclei was observed, probably deriving from ordered structures, persisting in the melt, and originated from the single crystals thickening process during the polymer dynamic melting in the DSC. © 2011 Wiley Periodicals, Inc. J Appl Polym Sci 123: 2697–2705, 2012

Key words: poly(L-lactide); crystallization; melting conditions; nucleation; memory effects; differential scanning calorimetry (DSC)

INTRODUCTION

The nucleation mechanism involved in poly(L-lactide) (PLLA) crystallization is a widely studied issue. In fact, PLLA is characterized by a slow crystallization kinetics and, under the high cooling rate usually used in molding processes, the crystallization could not takes place and glassy amorphous material is obtained. On the other hand, the dispersion of nucleating agents in the polymer melt represents wide industrial practice that enables the reduction of the crystallization induction period, the increase of the solidification rate and temperature, the control of the spherulite density and mean size and the final product crystallinity. Studies on different nucleating agents for PLLA, including poly(D-lactide) (PDLA),[1,2] modified clays,[3] talc,[2] ethylene bisstearamide (EBS),[4] 1,3,5-Benzenetricarboxylamide derivatives,[5] hydrazide compounds,[6] polyglycolide,[7] and self- nuclei,[2] were reported in literature.

In particular, Schmidt and Hillmyer,[2], according to the method proposed by Fillon et al.[8], compared the efficiency of heterogeneous nucleating agents with that of self nuclei, obtained by subjecting PLLA to different melting conditions. They found that the nucleation efficiency of stereocomplex crystallites formed in PLLA/PDLA blends, containing low concentrations of PDLA, was largely dependent on the thermal treatment of the melted sample.

The effect of the melting condition on the subsequent nonisothermal melt-crystallization was also studied by Wang and Mano[9], who related the double crystallization process, observed by DSC analysis, to the different nucleation mechanisms activated at different temperature. Other studies evidenced the presence of crystallization nuclei in the quenched amorphous PLLA. From isothermal and nonisothermal cold-crystallization experiments, it was found that their concentration depends on the cooling rate from the melt[10] and on annealing processes the amorphous polymer undergoes just above or below its glass transition temperature[11].

In general, it was observed that the presence and the concentration of heterogeneous nuclei or self-nuclei directly affect the crystallization process and, thus, the morphological mechanical, thermal, optical properties of the polymer products.

In the Part I of this article, we showed that the concentration of athermal nuclei directly influences the nonisothermal crystallization behavior of PLLA and indirectly the polymer structure.[12] By modulating the thermal treatment of the polymer in the melt state, we were able to vary the concentration of residual crystals fragments (self-nuclei) coming

Correspondence to: A. Martinelli (andrea.martinelli@uniroma1.it).

from the incomplete melting. Such ordered domains control, in subsequent cooling, the self-nucleation process.

The use of PLLA single crystals grown from dilute solution as starting standard material for our memory effect investigation allow us to completely erase the previous polymer thermal history and to obtain a crystalline homogeneous sample characterized by a very low concentration of foreign solid nuclei. By this way, we can clearly differentiate the predetermined and the sporadic nucleation mechanism.

The phenomena observed in our experiments showed that as the dwelling temperature of the polymer in the melt state, T_s, approaches the upper temperature limit of the self-nucleation range (named Domain II, after Fillon et al.), there is a selection of few stable self-nuclei, characterized by a narrow size distribution, which abruptly disappears at 188°C.[12] The great difference in the temperature dependence between the PLLA spherulitic growth rate [$G(T)$] and nucleation rate [$\dot{N}(T)$] and the low concentration of foreign heterogeneous nuclei favor the appearance of the double crystallization process starting from predetermined and sporadic nuclei.

Moreover, at the lowest nuclei concentrations, the self-nucleated crystallization takes place in the temperature region where the well-known change in PLLA crystal growth kinetics has been recorded, and a triple transition, occasionally observed by some authors, was interpreted.

In this article, to better understand these phenomena, we have analyzed in detail the DSC crystallization data. We made use of Nakamura-Avrami equation to model the PLLA nonisothermal crystallization kinetics and to follow the predetermined nuclei concentration as a function of the polymer thermal history.[13]

EXPERIMENTAL

Materials and methods

Poly(L-lactide) (M_n = 99,000, M_w = 152,000, Fluka) single crystals grown from 0.25% *p*-xylene polymer solution at $T_c^{sol} = 75$°C, were chosen as standard starting material to follow the effect of the thermal history in the melt state on the subsequent crystallization process. The detailed sample preparation procedure was reported in the Part 1 of this article.[12]

The Mettler DSC822^e differential scanning calorimeter (DSC) was used to subject the polymer to the desired thermal treatment and to record the nonisothermal melt crystallization process during the cooling at 5°C min^{-1}. The DSC scans were performed under nitrogen atmosphere on about 3 mg of powder form PLLA single crystals sealed in aluminum pans.

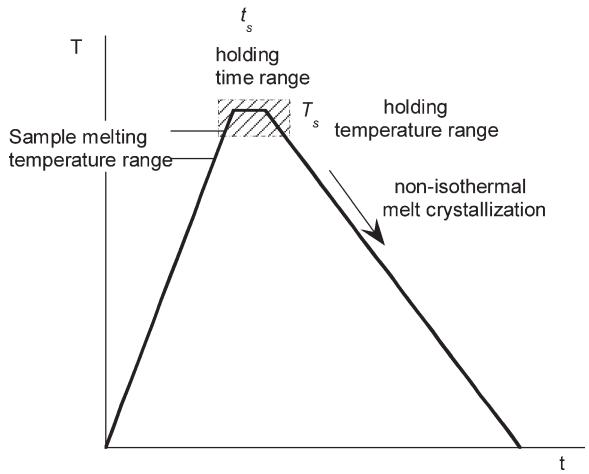

Figure 1 Schematic representation of temperature program used to study the effect of dwelling temperature (T_s) and time (t_s) of the polymer in the melt state on nonisothermal crystallization (cooling rate 5°C min^{-1}).

In Figure 1 the schematic temperature program against time is reported.

The samples were first heated at 10°C min^{-1} above the melting temperature and hold at a dwelling temperature (T_s) in the range 180–190°C for 5 min. For the samples treated at 187°C a holding time $0 \leq t_s \leq 45$ min was also analyzed. The sample was then cooled at 5°C min^{-1} to 25°C to record the crystallization process. This is the higher scanning rate which can be used without the incomplete crystallization occurs.[14] Lower cooling rates were not investigated to minimize any structural reorganization of the melt during the time period between the end of the thermal history of the polymer in the melt state and the crystallization onset.

The different temperature programs used in some experiments were described in the results discussion.

Theoretical framework

To study the variation of the nonisothermal crystallization kinetic parameters as a function of the thermal history of the polymer in the melt state, the overall crystallization process recorded by DSC at 5°C min^{-1} cooling rate was analyzed according to the Nakamura-Avrami model, a consolidate model discussed in detail and applied by a number of authors.[13,15,16] It reads as follows:

$$X_{DSC}(T) = 1 - \exp\left[-\left(\int_{T_0}^{T} Z(T)\frac{dT}{\dot{T}}\right)^n\right] \quad (1)$$

where $X_{DSC}(T)$ is the degree of phase transformation at temperature T evaluated from the nonisothermal melt crystallization thermograms according to:

$$X_{DSC}(T) = \frac{\int_{T_i}^{T} \frac{dH_c}{dT} dT}{\int_{T_i}^{T_f} \frac{dH_c}{dT} dT}; \quad (2)$$

$\dot{T}$ is the cooling rate, n the Avrami coefficient and $Z(T)$ is related to the Avrami rate constant $K(T)$ through the relation $Z(T) = [K(T)]^{1/n}$.

In the case of predetermined (athermal) nucleation mechanism and tridimensional crystalline aggregate formation, the Avrami rate constant is defined by the Equation:

$$K_{ath}(T, T_d, t_d) = \frac{4}{3}\pi \frac{\rho_S}{\rho_L} N_0(T, T_s, t_s) G(T, T_s, t_s)^3 \quad (3)$$

where $\rho_S/\rho_L \approx 1$ is the ratio between solid and liquid phase densities, $G(T, T_s, t_s)$ the spherulitic radial growth rate and $N_0(T, T_s, t_s)$ the number of predetermined active nuclei per unit of volume. Equation (3) represents the most general model, in which both the predetermined nuclei concentration and the growth rate depend on the temperature at which the crystallization takes place (T) and on the thermal history (T_s, t_s).

As far as the primary nucleation is concerned, we can consider that the macromolecular aggregates, coming from incompletely melted crystalline residues, are characterized by a size distribution depending only on the polymer thermal history above T_m. It means that, during the sample cooling, the low polymer mobility does not allow the attainment of a new size distribution or, in other terms, the relaxation time correlated to the redistribution of cluster size (equilibration) is longer than the external condition change (cooling). So, in a nonisothermal process, if the temperature range at which the crystallization takes place does not change too much with the thermal history, the dependence of N_0 on T may be neglect [$N_0 = N_0(T_s, t_s)$].

As far as the spherulite radial growth rate is concerned, generally it was considered independent of the melting condition used before the crystallization. Actually, the effect of the thermal history on the crystal growth has been observed, to the authors' knowledge, in a limited number of studies concerning the behavior of samples characterized by a low chain entanglement density, like single crystals and chain-extended crystals.[17,18] In both articles, it was observed that the spherulitic linear growth rate and the sample crystallinity decrease as the holding time or temperature in the melt state increase. These observations were interpreted in terms of entanglements creation during melting that obstacle the chain diffusion, slowing down the crystallization rate and decreasing the final crystallinity.

By introducing the Hoffmann-Lauritzen expression for $G(T)$, eq. (3) may be rewritten as:

$$K_{ath} = K^0_{ath} \exp\left\{ \left[\frac{-U^*}{R(T - T_\infty)} \right] \exp\left[-\frac{K_g}{T\Delta T f} \right] \right\}^3 \quad (4)$$

where $\Delta T = T^0_m - T$ is the supercooling, T^0_m the equilibrium melting temperature, U^* the activation energy for segment diffusion to the site of crystallization, R the gas constant, $T_\infty = T_g - 30$ is the temperature at which all chain motions associated with viscous flow cease, $f = 2T/(T + T^0_m)$ is a correcting factor taking into account the melting enthalpy variation with temperature and K_g is the secondary nucleation constant, dependent on the crystal growth regime, and

$$K^0_{ath} = \frac{4}{3}\pi \frac{\rho_S}{\rho_L} N_0(T_s, t_s) G_0^3 \quad (5)$$

is a constant proportional to predetermined active nuclei concentration.[19]

RESULTS AND DISCUSSION

As reported in the Part 1 of this article, the nonisothermal melt crystallization process of PLLA single crystals is greatly affected by the melting condition, defined as the polymer holding temperature (T_s) and time (t_s) in the melt state.[12]

The contour plots of DSC exothermic heat flow recorded during nonisothermal melt crystallization as a function of T_s (t_s = 5 min) and t_s (T_s = 187°C) are reported in Figure 2(A,B), respectively.

From the DSC and polarized optical microscopy observation, the different thermal behavior was ascribed to the different nucleation mechanism ruling the crystallization processes. At t_s = 5 min and $T_s \leq 186$°C the ordered domains survived in the melt act as predetermined nuclei and the polymer crystallizes at low supercooling (T^H_c). AT $T_s \geq 188$°C all the active nuclei are destroyed and sporadic nucleation takes place at high supercooling (T^L_c = 114°C). At the intermediate T_s ($187 \leq T_s \leq 187.5$°C) a mixed nucleation mechanism occurs. The transition temperature range $187 \leq T_s \leq 187.5$°C at which the crystallization mechanism change occurs was indicated by the dotted lines in Figure 2(A).

As expected, the high temperature range in which the crystallization takes place evidences the high efficiency of the residual aggregate as nucleating agent.[8]

In the experiments carried out at the fixed T_s = 187°C and different t_s [Fig. 2(B)], the double nucleation mechanism starts at t_s = 5 min and persists up to 45 min.

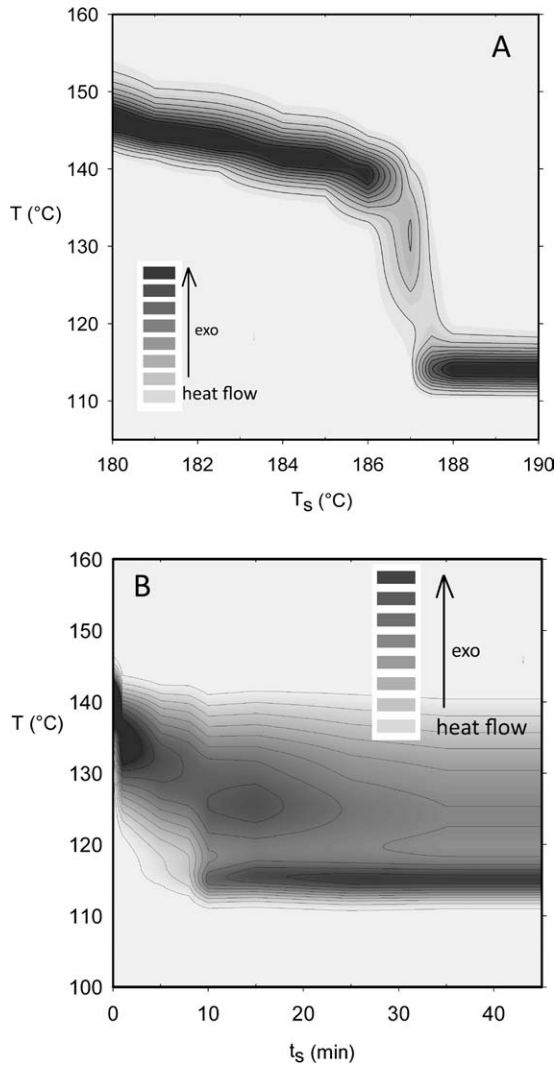

Figure 2 Contour plots of DSC cooling thermograms of PLLA samples held in the melt state at the indicated temperature T_s ($t_s = 5$ min) (line intervals 0.07 W g^{-1}) (A) and time t_s ($T_s = 187$°C) (line intervals 0.06 W g^{-1}) (B).

In preliminary experiments carried out in this research on PLLA single crystals (results not reported), we found that the isothermal spherulitic growth rate G was not greatly affected by the melting condition in the range $180 < T_s < 187$°C and that the effect of the athermal nuclei concentration change greatly overwhelms the G variation in the overall crystallization kinetics. In our case the dependence of G on T_s and t_s may be neglected, that is, in eq. (3), $G = G(T)$.

Equations (1), (3), and (4) were used to interpolate the DSC data recorded at $180°C \leq T_s \leq 187°C$, that is in the temperature range where the predetermined nucleation mechanism occurs.

To find reliable values of the parameters K^0_{ath}, K_g, and n by a least squares fitting procedure of the experimental results, it was necessary to chose suitable starting input values.

According to the optical microscopy experiments reported in the previous paper, where instantaneous nucleation and spherulitic growth were observed, an Avrami coefficient $n = 3$ was initially fixed. On the other hand n value close to 3 was also obtained by a number of authors in isothermal crystallization experiment carried out on self-nucleated or heterogeneously nucleated PLLA.[1,2]

As far as the K_g parameter is concerned, we started with $K_g = 3 \times 10^5$, one of the values reported in the literature.[1,20] The values $T^0_m = 480$ K, $U^* = 6.28$ kJ $mole^{-1}$, and $T_\infty = T_g - 30 = 308$ K were used in eq. (4).[21]

Whereas the polymer thermal treatment in the melt state is mild ($180°C \leq T_s \leq 186°C$), the crystallization takes place in the 135–145°C range, that is far away from the temperature at which an apparent change in the crystallization regime II-III was recorded (115–120°C).[22,23] So, assuming that K_g does not vary with the thermal treatment, the optimization of this parameter was carried out contemporarily for all the experimental data set collected at different T_s. Once the K^0_{ath} and K_g parameters were obtained, no appreciable change from $n = 3$ was observed when the n value was allowed to vary freely in the fitting. If other Avrami coefficients are used as starting input ($n = 1$, 2, or 4), unrealistic K_g, T^0_m, and T_∞ values are necessary to obtain acceptable data interpolations.

Figure 3 shows the experimental $X_{DSC}(T)$ data as a function of T for the different T_s ($t_s = 5$ min) and the best fit curves according to Nakamura model [eq. (1), (3), and (4)].

The model fits very well the experimental results in the range $0.2 \leq X_{DSC}(T) \leq 0.8$. The K_g value was estimated to be $(4.4 \pm 0.5) \times 10^5$ K^2, lightly higher

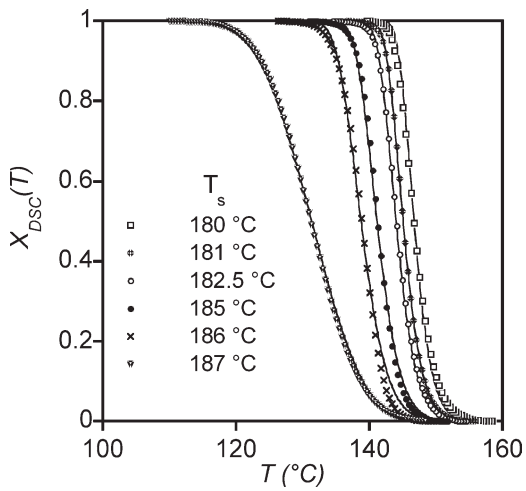

Figure 3 DSC crystalline conversion degree $X_{DSC}(T)$ as a function of temperature for PLLA samples held at the different indicated T_s. The curves represent the best fit according the Nakamura-Avrami model [eq. (1), (3), and (4)].

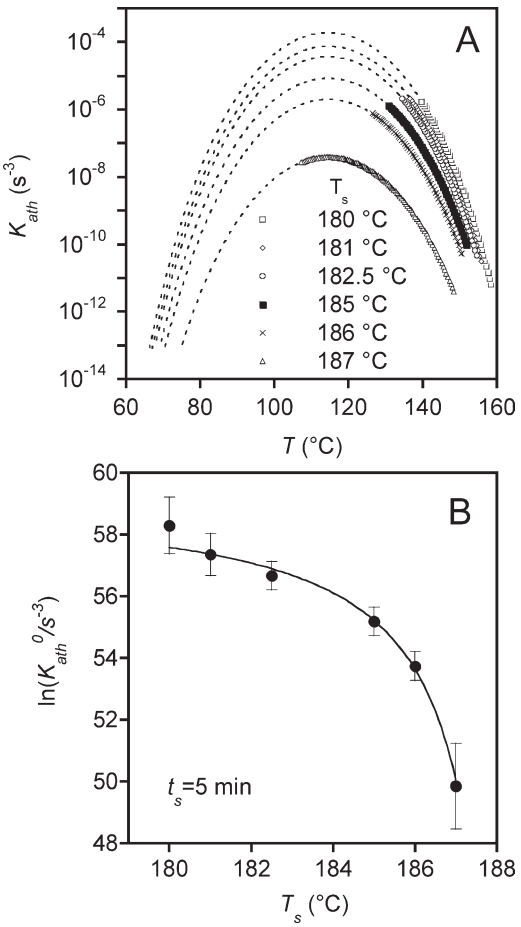

Figure 4 Variation of K_{ath} calculated by employing the best fit parameters in the crystallization (dots) and in the extrapolated wider (lines) temperature range (A). Influence of the holding temperature on K^0_{ath}, proportional to the nuclei concentration N_0 (B).

than the values reported in literature for isothermal experiments.[21,22] Such a small deviation may arise from the imperfect prediction of the nonisothermal experiments by using isothermal data, due to the different thermal lag associated to the two crystallization conditions.

In Figure 4(A) are reported the K_{ath} data calculated by using the best fit parameters in the crystallization (dots) and in the extrapolated wider temperature range (dotted lines).

The different curves represent the temperature dependence of $[G(T)]^3$ scaled by the preexponential term of eq. (4), proportional to the predetermined nuclei concentration, $N_0(T_s,t_s)$ [eq. (3)]. The effect of the melting temperature on $K^0_{ath} \propto N_0(T_s,t_s)$ is shown in Figure 4(B).

It may be observed that by increasing the T_s from 180 to 187°C, a reduction of predetermined nuclei concentration of about 5 orders of magnitude is recorded. Similar N_0 drop over a small melting temperature range was observed by other authors both in PLLA and iPP samples.[2,8]

In a first approximation, the K^0_{ath} value could be associated to the mean nuclei disappearance rate within the constant isothermal melting time (5 min) compared with an initial ($t_s = 0$) fixed nuclei concentration. According to this hypothesis, the K^0_{ath} data versus T_s may be conveniently interpolated by the Tamman-Vogel-Fulcher (TVF) relation:

$$K^0_{ath} = K^{00}_{ath} \exp\left(-\frac{A}{T^0_s - T_s}\right) \quad (6)$$

where K^{00}_{ath} and A are constants and T^0_s represents the temperature at which the number of predetermined active nuclei diverges, that is the limiting extrapolated temperature at which the system looses all the previous crystalline state memory. The fitting gives a $T^0_s = 189°C \pm 1°C$. This value practically coincides with the observed experimental melting temperature $T_s = 188°C$ above which the subsequent crystallization follows essentially a sporadic nucleation mechanism. Interestingly, the upper $T^0_s = 190°C$ value coincides also with the temperature T_0 determined by linear extrapolation of melting, recrystallization and crystallization lines, as obtained by Cho and Strobl by reporting the inverse crystal thickness d_c of melt crystallized PLLA versus the crystallization, recrystallization and melting temperature.[24] The authors referred to T_0, or to a temperature close to it, as a sort of a triple point where the mesomorphic, the amorphous and the crystalline phases coexist.

In our experiments, we could follow the polymer melting process up to temperature very close to the limiting value T^0_s, determined by using a negligible extrapolation. The crystallization process, in fact, is an indirect but very sensitive tool to characterize the melting state, able to detect the presence of ordered structures, otherwise hard to observe or invisible to the usual experimental techniques.[25]

A clear evolution of the crystallization process was also observed as a function of the melting time (t_s) at $T_s = 187°C$. The DSC profile changes up to about $t_s = 10$–15 min [Fig. 2(B)] and then it does not undergo any further modification at longer dwelling time, revealing the existence of an equilibrium concentration in the time period investigated of predetermined nuclei that were not destroyed by the thermal treatment above the melting temperature. Because of the progressive reduction of the nuclei number, the crystallization process from self-nuclei slows down and partially takes place in a temperature range below 120°C. At this temperature it has been observed a crystallization kinetics change initially attributed to a variation of the crystallization regime from II to III or, more recently, to the different grow rate of the two possible PLLA crystalline modification α and α′, stable at $T > 120°C$ and

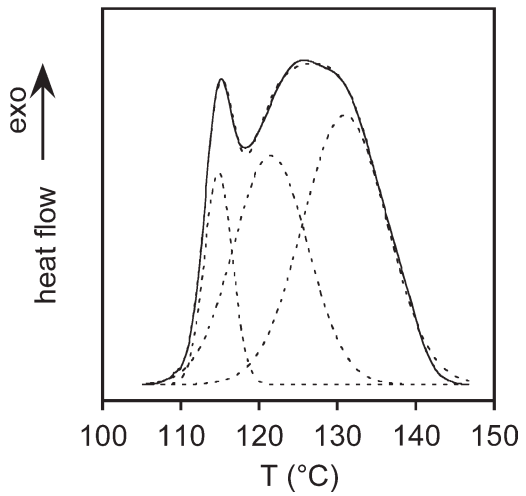

Figure 5 DSC cooling thermogram of PLLA sample dwelled at $T_s = 187°C$ for $t_s = 15$ min (solid line). The dashed lines show the Gaussian functions used to decompose the crystallization curve and their sum.

$T < 120°C$, respectively.[20,22] This involves that the parameter $K_g = 4.4 \times 10^5$ s^{-3} previously employed cannot be used and that the proportionality factor G_0^3 between K_0^{ath} and N_0 changes [eq. (5)]. The variation of the secondary nucleation constant K_g at about 120°C leads to a crystallization DSC profile modification. As shown in Figure 5, where the cooling thermogram of the $T_s = 187°C$ $t_s = 15$ min sample is reported as an example, the whole exothermal transition is composed by three overlapped process, here well approximated by three Gaussian functions.

The processes at higher and intermediate temperature represent the crystallization initiated by predetermined nuclei taking place with the two different grow rates. The lower temperature one represents the crystallization with the homogeneous nucleation mechanism. This interpretation was supported by the fact that the higher and intermediate temperature crystallization data may be independently fitted by Nakamura model [eq. (1), (3), and (4)] by using $K_g^{II} = 4.4 \times 10^5$ K^2 and $K_g^{III} = 8.2 \times 10^5$ K^2. The ratio $K_g^{III}/K_g^{II} = 1.82$ is rather close to the value 2 predicted by the theory and found by a number of authors.[1,20,22]

To avoid entangled model equations taking into account both the crystallization kinetics with a higher adjustable parameter number, we decided to use the same fitting procedure and starting parameters previously described, into a restricted temperature range. The predetermined crystallization process was separated from the homogeneous one by subtracting from the total DSC profile the lowest temperature Gaussian curve. For the $t_s \geq 8$ min samples, the conversion degree, obtained from eq. (2), was truncated at $T < 125°C$.

A good fitting of the whole ($0 \leq t_s \leq 5$ min) or selected ($8 \leq t_s \leq 45$ min) crystallization data was obtained by fixing $n = 3$ and $K_g = 4.4 \times 10^5$ K^2. Figure 6 shows the effect of the dwelling time on the K_{ath}^0 values.

The K_{ath}^0 value, proportional to the predetermined nuclei concentration, exponentially decreases with increasing t_s till about 10 min and then it levels off at a finite value. The experimental data were interpolated by using the eq. (7), based on a modification of the Alfonso and Ziabicky model[26]:

$$K_{ath}^0 = K_{ath}^{0f} + (K_{ath}^{0i} - K_{ath}^{0f})^* \exp(-t_s/\tau) \qquad (7)$$

where K_{ath}^{0i} and K_{ath}^{0f} are the initial ($t_s = 0$) and final extrapolated ($t_s = \infty$) K_{ath}^0 values and τ the relaxation time related to the cluster size redistribution (equilibration) at $T_s = 187°C$. The curve fit gives the following values: $K_{ath}^{0i} = 4.1 \times 10^{22}$ s^{-3}, $K_{ath}^{0f} = 1.2 \times 10^{21}$ s^{-3}, and $\tau = 115$ s.

The t_s variation was found to have a much lower influence on the nonisothermal crystallization of PLLA single crystals than the melting temperature change. At $T_s = 188°C$, a melting time period of 1 min is sufficient to erase all the sample crystalline memory. On the other hand, at $T_s \leq 186°C$, no substantial modification of crystallization temperature (T_c) or DSC profile were recorded by varying t_s from 0 to 45 min (data not reported). Therefore, the very narrow temperature range in which it is possible to investigate the variation of nuclei concentration as a function of the dwelling time precluded the knowledge of the dependence of τ versus T_s and, then, any activation energy calculation.[26]

The $K_{ath}^{0f} \neq 0$ means that a steady concentration of ordered clusters survives in the melted polymer at 187°C, that is at a temperature 4°C higher than that of the polymer melting process completion at 183°C, where the DSC baseline is recovered after the melting endotherm.

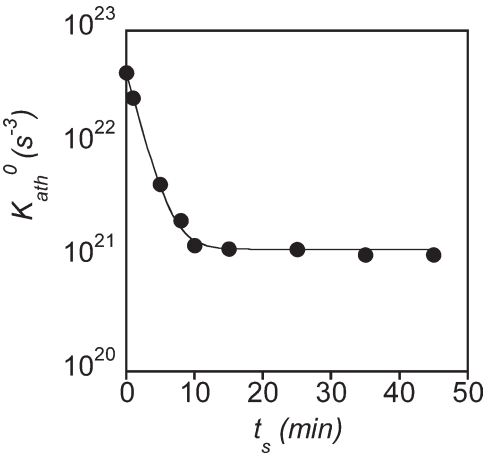

Figure 6 K_{ath}^0 variation as a function of the holding time t_s at $T_s = 187°C$. The experimental data were fitted by eq. (6) (solid line).

It is possible to make some conjectures about nature and the origin of such nuclei.

In the original model proposed by Alfonso and Ziabicky, the predetermined nuclei equilibrium concentration at infinite melting time is exclusively assigned to infusible heterogeneous particles.[26]. In our case, they cannot be foreign nuclei, being readily destroyed at a melting temperature just 1°C higher.

They could originate from stable crystal fragments survived to the melting process and not detected by DSC because of their low concentration.

Alternatively, the existence of potential nuclei could arise from an equilibrium concentration of subcritical size clusters at $T>T_m$. The effect of such cluster on the crystallization process may be observed in the absence of heterogeneous nucleation and when the gradual melting of the instable nuclei from the previous crystal structure ceases (in our case when $t_s \gg \tau$). Ziabicki and Alfonso, exclude this possibility for organic polymer because of the high value of the $\sigma/\Delta H_m$ ratio, being σ the average surface energy and ΔH_m the heat of melting: the self-nuclei surviving above the melting temperature are not in equilibrium state and the isotropic melt may be achieved by using an appropriate long residing time, dependent on the melting temperature.[25,27–29]

However, some authors report the possible presence in the polymer melt of ordered structures, referred as bundles, partially ordered melt, LCP-like structured liquid, helical regularity structures, anisotropic domains according to interpretation of experimental results. Such structures have been evidenced by DSC, torque measurements, FTIR, NMR, and small angle light scattering (SALS).[30–34].

According to Janeshhitz-Kriegl, structures similar to the "fringed micelle," formed by occasional lateral association of few strands of proper helical conformation, may exist in the metastable melt, i.e., at temperature below the thermodynamic melting point.[35] Their stability arises from the fact that the few tangling ends that freely emanate in the melt are characterized by a low end surface free energy (σ_e) value. σ_e increases as the lateral dimension of such bundle type nuclei increases through the further strand deposition, till a constant saturation value is reached in the chain folded lamella.

To evaluate the possible presence of an equilibrium nuclei concentration in the melt state, independent from the thermal history and from the starting sample structure, PLLA single crystals were first heated for 5 min at $T_s = 190$°C, temperature at which the nuclei were completely destroyed, and then annealed at 187°C for 15 min. The crystallization process was then recorded by using the usual 5°C min^{-1} cooling rate. In this case the crystallization peak is found at $T_c = 114$°C, indicating a sporadic nucleation [Fig. 2(A)]: no new clusters are formed when the homogeneous melt where dwelled at 187°C, a temperature otherwise not sufficient for the complete melting during the sample heating.

The presence of stable structure derived by the sample incomplete melting at $T_s \leq 187$°C seems to be strictly related to the use of single crystals as starting sample. In fact, if we impose to the sample two successive melting-crystallization cycles described in Figure 1, respectively, at $T_s = 190$°C ($t_s = 5$ min) (memory erasing and isotropic melt attainment) and $T_s = 187$°C ($t_s = 5$ min), the second nonisothermal crystallization process takes place at $T_c = 114$°C, that is with sporadic nucleation.

Moreover, Schmidt and Hillmayer observed that, for starting PLLA samples nonisothermally crystallized from the melt at 210°C, a thermal treatment at just 183°C is sufficient to completely erase any memory of the previous crystalline structure.[2] The self-nucleation phenomenon was recorded at lower melting temperature. The residual number of nuclei observed at $T > 183$°C by the authors was attributed to heterogeneous contaminants.

The thermal stability up to 187°C of the crystalline aggregates we observed may be imputed to the PLLA single crystals reorganization process that takes place during the DSC first heating scan. In fact, Fujita and Doi, by means of *in situ* temperature-controlled atomic force microscopy (AFM) analysis, directly observed that, during annealing from 126°C, the PLLA single crystals (original thickness 11–12 nm) undergo a complex thickening process starting from the lamellae edges.[36] At the highest explored annealing temperature (168°C), single crystal regions up to 20–30 nm have been observed. The effect of annealing on the single crystal morphology was also investigated by Miyata and Masuko.[37] They reported that erratic thickening and surface roughening of the single crystals take place just below the melting point (180°C), where a lamellar thickness of about 22–23 nm was measured by AFM. By means of temperature-dependent SAXS experiments, Cho and Strobl, starting from melt crystallized PLLA, recorded a crystal thickening up to 20 nm before the melting point at 170°C.[24]

The Thompson-Gibbs equation may be used to establish a correlation between the melting temperature T_m and the crystalline thickness l:

$$T_m = T_m^0\left(1 - \frac{2\sigma_e}{l\Delta H_m^0}\right) \tag{8}$$

where $T_m^0 = 480$°C, $\sigma_e = 40.5$ erg cm^{-2} is the PLLA free energy of folding and $\Delta H_m^0 = 1.11 \times 10^8$ J m^{-3} the PLLA enthalpy of fusion.[21,22] By using in eq. (8) the value $T_m = 188$°C (460 K), temperature at which we observed the isotropic melt achievement, an $l = 17.5$ nm is obtained. Lightly different results were

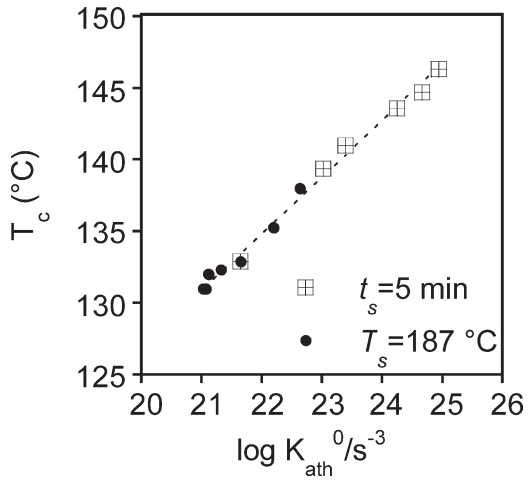

Figure 7 Effect of K_{ath}^0, proportional to the nuclei concentration N_0 [see eq. (5)], on the nonisothermal crystallization temperature T_c.

obtained by using different parameter values reported in literature. As a consequence of the approximation contained in the Thompson-Gibbs equation, where the lateral free energy contribution is neglected, this value may be considered just as a thickness estimation of the crystalline aggregates survived in the melt, precursor of the self-nucleation process. Actually, a large lateral surface may be expected for the small crystal clusters dispersed in the melt phase. In any case, by taking into account the amorphous folding surface layer contribution to the total thickness, the $l = 17.5$ nm value is in good agreement with the AFM and SAXS measurements.

The presence and the concentration of residual crystal fragments in the melt, by reducing the energy barrier for the crystallization process, increases the temperature at which the crystallization takes place in dynamic cooling. To correlate all the results relevant to the self-nucleation experiment carried out at different T_s ($t_s = 5$ min) and t_s ($T_s = 187$°C) we reported in Figure 7 the dependence of crystallization DSC peak temperature T_c as a function of K_{ath}^0, proportional to the athermal nuclei concentration. For the experiment carried out at $T_s = 187$°C and $t_s \geq 8$ min, the peak temperature of the higher temperature Gaussian function was taken.

The Figure 7 shows that the crystallization temperature directly depends solely on the nuclei concentration and not on the sample thermal history. Moreover, all the data fall into a straight line only when the change in crystallization mechanism or in the growth rate is absent.

According to the prediction based on the Eder crystallization model, a linear dependence of the logarithm of nuclei concentration as a function of the crystallization temperature was also observed by Fillon et al.[12]

CONCLUSIONS

The effect of the melting condition on PLLA nonisothermal crystallization kinetics showed to be a powerful tool to characterize the polymer melt state. In the memory effect experiment here reported the use of single crystals grown from dilute solution as starting standard material enlightened some interesting phenomena concerning the presence and the nature of ordered crystallization precursor in the polymer melt phase.

The low number or the absence of infusible heterogeneous nuclei in our system allowed us to follow the self-nuclei concentration decrease with increasing the melting temperature to a limiting null value at an holding temperature $T_s = 190$°C. At this holding temperature the subsequent nucleation is purely sporadic.

Moreover, it was observed that there is a very narrow temperature range, around 187°C, that is above melting temperature where the DSC baseline is recovered after the melting endotherm, at which the concentration of self-nuclei decays as a function the melting time, approaching to an equilibrium value. The presence in the melt of such structures was shown to be strictly related to the thickening phenomenon the single crystals undergo during the starting sample heating process.

Finally, the complex PLLA nonisothermal crystallization, occasionally observed as a triple transition, was interpreted. At low self-nuclei concentration, the crystallization process initiated by predetermined nuclei takes place with two different growth rates (higher and intermediate temperature endothermic DSC overlapped peaks). The lower temperature DSC peak represents the crystallization with the homogeneous nucleation mechanism.

References

1. Tsuji, H.; Takai, H.; Saha, S. K. Polymer 2006, 47, 3826.
2. Schmidt, S. C.; Hillmyer, M. A. J Polym Sci Part B: Polym Phys 2001, 39, 300.
3. Krikorian, V.; Pochan, D. J. Macromolecules 2005, 38, 6520.
4. Harris, A. M.; Lee, E. C. J Appl Polym Sci 2008, 107, 2246.
5. Nakajima, H.; Takahashi, M.; Kimura, Y. Macromol Mater Eng 2010, 295, 460.
6. Kawamoto, N.; Sakai, A.; Horikoshi, T.; Urushihara, T.; Tobita, E. J Appl Polym Sci 2007, 103, 198.
7. Tsuji, H.; Tashiro, K.; Bouapao, L.; Narita, J. Macromol Mater Eng 2008, 293, 947.
8. Fillon, B.; Wittmann, J. C.; Lotz, B.; Thierry, A. J Polym Sci Part B: Polym Phys 1993, 31, 1383.
9. Wang, Y.; Mano, J. F. Eur Polym Mater 2005, 41, 2335.
10. Sánchez, M. S.; Mathot, V. B. F.; Poel, G. V.; Gómez Ribelles, J. L. Macromolecules 2007, 40, 7989.
11. Sánchez, F. H.; Mateo, J. M.; Colomer, F. J. R.; Salmeron Sánchez, M.; Gómez Ribelles, J. L.; Mano, J. F. Biomacromolecules 2005, 6, 3283.
12. Martinelli, A.; Calì, M.; D'Ilario, L.; Francolini, I.; Piozzi, A. J Appl Polym Sci 2011, 121, 3368.

13. Nakamura, K.; Katayama, K.; Amano, T. J Appl Polym Sci 1973, 17, 1031.
14. Salmeron Sanchez, M.; Gomez Ribelles, J. L.; Hernandez Sanchez, F.; Mano, J. F. Thermochim Acta 2005, 430, 201.
15. Patel, R. M.; Spruiell, J. E. Polym Eng Sci 1991, 31, 730.
16. Martins, J. A.; Cruz Pinto, J. J. C. Polymer 2000, 41, 6875.
17. D'Ilario, L.; Martinelli, A.; Piozzi, A. J Macromol Sci Phys 2002, B41, 47.
18. Psarski, M.; Piorkowska, E.; Galeski, A. Macromolecules 2000, 33, 916.
19. Hoffman, J. D.; Davis, G. T.; Lauritzen, J. I. In Treatise on Solid State Chemistry;Hannay, N. B., Eds.; Plenum Press: New York, 1976; Vol.3,Chapter 7, pp 565–592.
20. Kawai, T.; Rahman, N.; Matsuba, G.; Nishida, K.; Kanaya, T.; Nakano, M.; Okamoto, H.; Kawada, J.; Usuki, A.; Honma, N.; Nakajima, K.; Matsuda, M. Macromolecules 2007, 40, 9463.
21. Vasanthakumari, R.; Pennings, A. J. Polymer 1983, 24, 175.
22. Di Lorenzo, M. L. Polymer 2001, 42, 9441.
23. Iannace, S.; Nicolais, L. J Appl Polym Sci 1997, 64, 911.
24. Cho, T.-Y.; Strobl, G. Polymer 2006, 47, 1036.
25. Maus, A.; Hempel, E.; Thurn-Albrecht, T.; Saalwachter, K. Eur Phys J 2007, 23, 91.
26. Alfonso, G. C.; Ziabicki, A. Colloid Polym Sci 1995, 273, 317.
27. Alfonso, G. C.; Ziabicki, A. Colloid Polym Sci 1994, 272, 1027.
28. Lorenzo, A. T.; Arnal, M. L.; Sanchez, J. J.; Muller, A. J. J Polym Sci Part B: Polym Phys 2006, 44, 1738.
29. Supaphol, P.; Spruiell, J. E. J Appl Polym Sci 2000, 75, 337.
30. Hussein, I. A.; Williams, M. C. Macromolecules 2000, 33, 520.
31. Hussein, I. A.; Williams, M. C. J Non-Newt Fluid Mech 1999, 86, 105.
32. Zhu, X.; Yan, D.; Yao, H.; Zhu, P. Macromol Rapid Commun 2000, 21, 354.
33. Graf, R. A.; Heuer, A.; Spiess, H. W. Phys Rev Lett 1998, 80, 5738.
34. Xiao, Z.; Akpalu, Y. A. Polymer 2007, 48, 5388.
35. Janeschitz-Kriegl, H. Colloid Polym Sci 2003, 281, 1157.
36. Fujita, M.; Doi, Y. Biomacromolecules 2003, 4, 1301.
37. Miyata, T.; Masuko, T. Polymer 1997, 38, 4003.